Bioconjugation

DOI: 10.1002/anie.201404616

A Chemoenzymatic Approach to Protein Immobilization onto Crystalline Cellulose Nanoscaffolds**

Christina Uth, Stefan Zielonka, Sebastian Hörner, Nicolas Rasche, Andreas Plog, Hannes Orelma, Olga Avrutina, Kai Zhang, and Harald Kolmar**

Abstract: *The immobilization of bioactive molecules onto nanocellulose leads to constructs that combine the properties of the grafted compounds with the biocompatibility and low cytotoxicity of cellulose carriers and the advantages given by their nanometer dimensions. However, the methods commonly used for protein grafting suffer from lack of selectivity, long reaction times, nonphysiological pH ranges and solvents, and the necessity to develop a tailor-made reaction strategy for each individual case. To overcome these restrictions, a generic two-step procedure was developed that takes advantage of the highly efficient oxime ligation combined with enzyme-mediated protein coupling onto the surface of peptide-modified crystalline nanocellulose. The described method is based on efficient and orthogonal transformations, requires no organic solvents, and takes place under physiological conditions. Being site-directed and regiospecific, it could be applied to a vast number of functional proteins.*

In recent years, the development of novel nanocellulose-based materials has attracted growing scientific interest. Since it is a major building block of the biosphere, cellulose is considered as a renewable natural resource and could become a substitute for nonrenewable synthetic polymers.[1] Cellulose-based new materials possess fascinating properties and have been used recently in a vast number of life-science and technical applications.[2]

Contributing to the expanding field of novel sustainable compounds, crystalline nanocellulose has been in the focus of various interdisciplinary studies.[3] Generally, cellulose nanocrystals (CNCs) or nanofibrils are formed upon elimination of amorphous parts from native cellulose fibers and can be prepared following different strategies, among them acid hydrolysis, microfluidization, and TEMPO-mediated oxidation (Figure 1 a).[3b,4] With a diameter of up to 20 nm and a length between 100 nm and 1 μm,[3b,4] CNCs have a significantly more expanded surface area than native cellulose, thus allowing for stronger multiple interactions. Moreover, they can be dispersed in diverse solvents, including water, rendering CNCs as a nanoscale substrate for the immobilization of various compounds that require physiological conditions for their proper function, among them DNA, proteins, and peptides.[5] The resulting constructs combine the properties of grafted compounds with the biocompatibility and low cytotoxicity of cellulose carriers[1,2a,6] and the advantages given by their nanosize.

The methods for protein immobilization onto nanocellulose surfaces can be broadly divided into three main groups according to the molecular forces that mediate binding: a) physical interactions between the protein and the particle surface; b) affinity interactions between the protein and the ligand; c) covalent interactions. In view of covalent protein immobilization two important issues have to be addressed: the preservation of the structural and dimensional properties of nanocellulose and the maintenance of the bioactivity of the immobilized biomolecule. Due to the inherent bioinertness of nanocellulose scaffolds, their surface requires activation or modification to enable interaction with the addressable sites within macromolecules.[5d–f,7] To this end, the free, superficial hydroxy groups are often transformed into the respective carboxylic acids by TEMPO-mediated oxidation, thus allowing for direct amide coupling or other further modifications.[5d,e,7a,b] To date, a number of peptides and proteins have been immobilized onto the surface of nanoscaled cellulose, for example, tryptophan-based oligopeptides comprising two to eight amino acid residues,[5b,c] a human neutrophil elastase tripeptide substrate,[5e] the enzyme alkaline phosphatase, and anti-hydrocortisone antibodies.[5d]

As the *N*-terminus and all surface-exposed lysine residues of proteins provide reactive amino groups, their linkage to the nanoparticle occurs in an uncontrolled fashion, which may result in the attachment at a site of the protein that affects its structure, stability, or bioactivity (see Figure S11 in the Supporting Information).[8] Therefore, several approaches have been developed to assure better selectivity and bioorthogonality, among them a noncovalent specific binding between an antibody of interest and its peptidic ligand coupled to the surface through a copolymer spacer[6b] and the

[*] Dr. H. Orelma, Dr. K. Zhang
Ernst-Berl-Institut für Technische und Makromolekulare Chemie
Technische Universität Darmstadt
Alarich-Weiss-Strasse 8, 64287 Darmstadt (Germany)
E-mail: zhang@cellulose.tu-darmstadt.de
A. Plog
Center of Smart Interfaces
Technische Universität Darmstadt (Germany)
C. Uth, S. Zielonka, S. Hörner, Dr. N. Rasche, Dr. O. Avrutina, Prof. Dr. H. Kolmar
Clemens-Schöpf-Institut für Organische Chemie und Biochemie
Technische Universität Darmstadt
Alarich-Weiss-Strasse 4, 64287 Darmstadt (Germany)
E-mail: kolmar@biochemie-tud.de

[**] We thank the Hessische Exzellenz Initiative LOEWE—Forschungscluster SOFT CONTROL and the Kooperative Forschungskolleg NANOKAT and DFG priority program 1623 for financial support and Brent Dorr (Harvard University) for providing the plasmid for the sortase expression.

Supporting information for this article is available on the WWW under http://dx.doi.org/10.1002/anie.201404616.

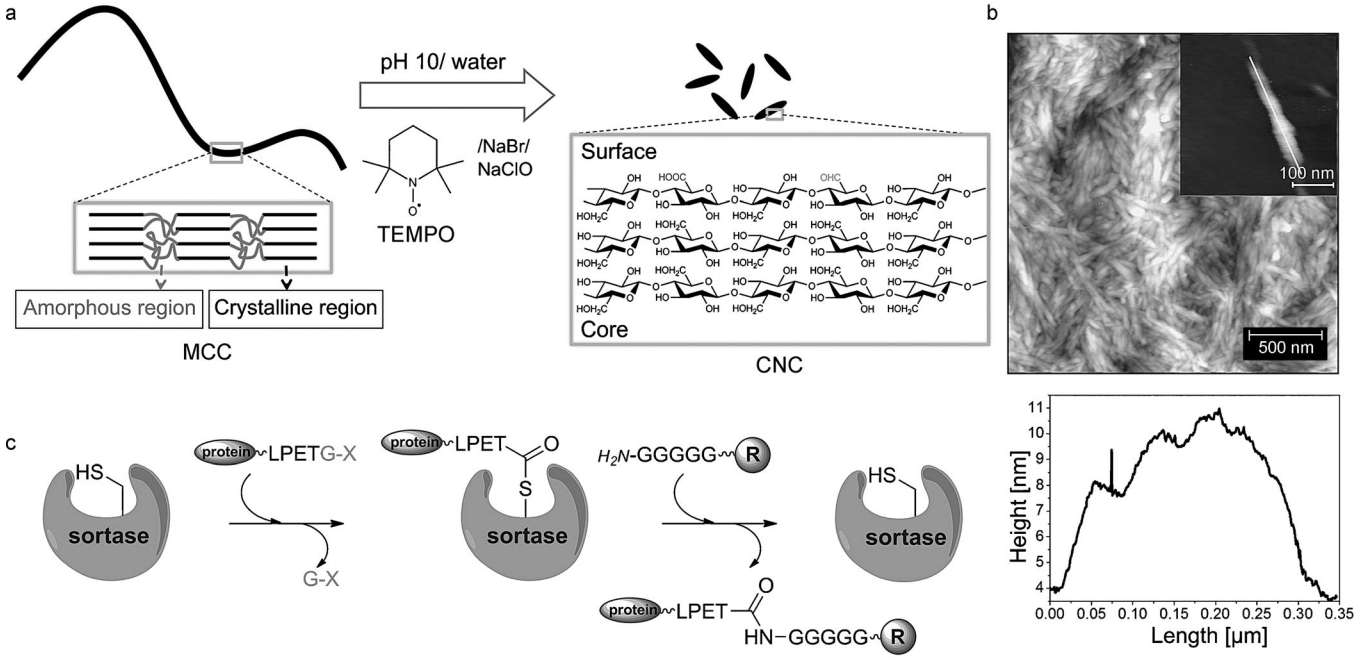

Figure 1. a) Schematic representation of the synthesis of CNCs from microcrystalline cellulose (MCC) through TEMPO-mediated oxidation. b) Top: AFM image of obtained CNCs. The inset presents the AFM image of a single CNC. Bottom: height profile. c) Illustration of sortase-mediated ligation. R represents the moiety of choice, X any amino acid. Amino acids are indicated as one-letter code with the amino terminus shown.

deposition of nanogold on polyethyleneimine-coated nanocellulose allowing for the functionalization with respective thiols.[7c] Site-specific azide–alkyne cycloaddition has been used for immobilization as well, but the reaction procedure was rather sophisticated and could not be applied to functional proteins.[7d] Although these approaches allowed the grafting of human immunoglobulin G (IgG),[5f] glucose oxidase,[9] and β-casein[7d] as well as avidin–biotin complexes, bovine serum albumin, and antihuman IgG[5f,10] onto nanocellulose scaffolds, the procedures suffer from lack of selectivity, long reaction times, nonphysiological pH ranges or solvents, and the necessity to develop a particular reaction strategy for each individual case. To overcome these restrictions, we decided to take advantage of enzyme-mediated biotransformations for covalent bioconjugations.[11]

Over the last decade, the transpeptidase sortase A found in Gram-positive bacteria (where it is used to covalently attach proteins to peptidoglycan layers) has emerged as a powerful tool for the modification of various nature-derived and engineered molecular constructs.[11b,c,12] This enzyme requires two short recognition sequences and generates a native amide bond upon ligation.

The ultimate goal of the present research was the covalent regioselective grafting of bioactive proteins on the surface of CNCs decorated with orthogonally addressable functionalities, for example, aldehyde units. In general, these groups provide the possibility to apply highly efficient and selective oxime ligation using the respective aminooxy function as a reaction partner.[13] Although this moiety can be easily introduced into oligopeptides, both on solid support and in solution, oximation has its highest turnover rate at nonphysiological pH (4–5). As most bioactive proteins lose their proper fold at these pH ranges, near-physiological pH should be applied, leading to prolonged duration of the oxime ligation. As a consequence, the conjugation of full-size proteins is obviously restricted. Therefore, we designed a peptidic linker that combined the required aminooxy function (allowing the prior attachment on CNCs) with a recognition sequence enabling enzyme-catalyzed protein ligation under physiological conditions.

For the anchoring of bioactive proteins on the CNC surface, sortase A mediated ligation was chosen (Figure 2). This calcium-dependent transpeptidase recognizes two short peptidic motifs, LPXTG and oligo-Gly, and catalyzes cleavage at the *C*-terminus of threonine (Figure 1c). Subsequent coupling to the *N*-terminus of the oligo-Gly partner results in a newly formed inter- or intramolecular amide bond, depending on the position of the recognition units. An oligo-Gly sequence was grafted onto the CNC surface, and an LPETG motif was genetically introduced into the respective protein counterparts (Figure 3).

CNCs were prepared from microcrystalline cellulose through TEMPO-mediated oxidation.[4a,14] During this two-step procedure, the primary hydroxy groups at the C6-position were converted into the respective aldehydes as precursors of carboxylic acids. The resulting CNC surface was decorated with both carboxy and aldehyde groups,[15] and their content was determined to be 1.386 mmol g^{-1} and 0.072 mmol g^{-1}, respectively (see Figure S1 and Section 1.3 in the Supporting Information). AFM measurements showed that the obtained CNCs had the form of whiskers with a diameter of around 7 nm and a length of around 300 nm (Figure 1b).[4c,16]

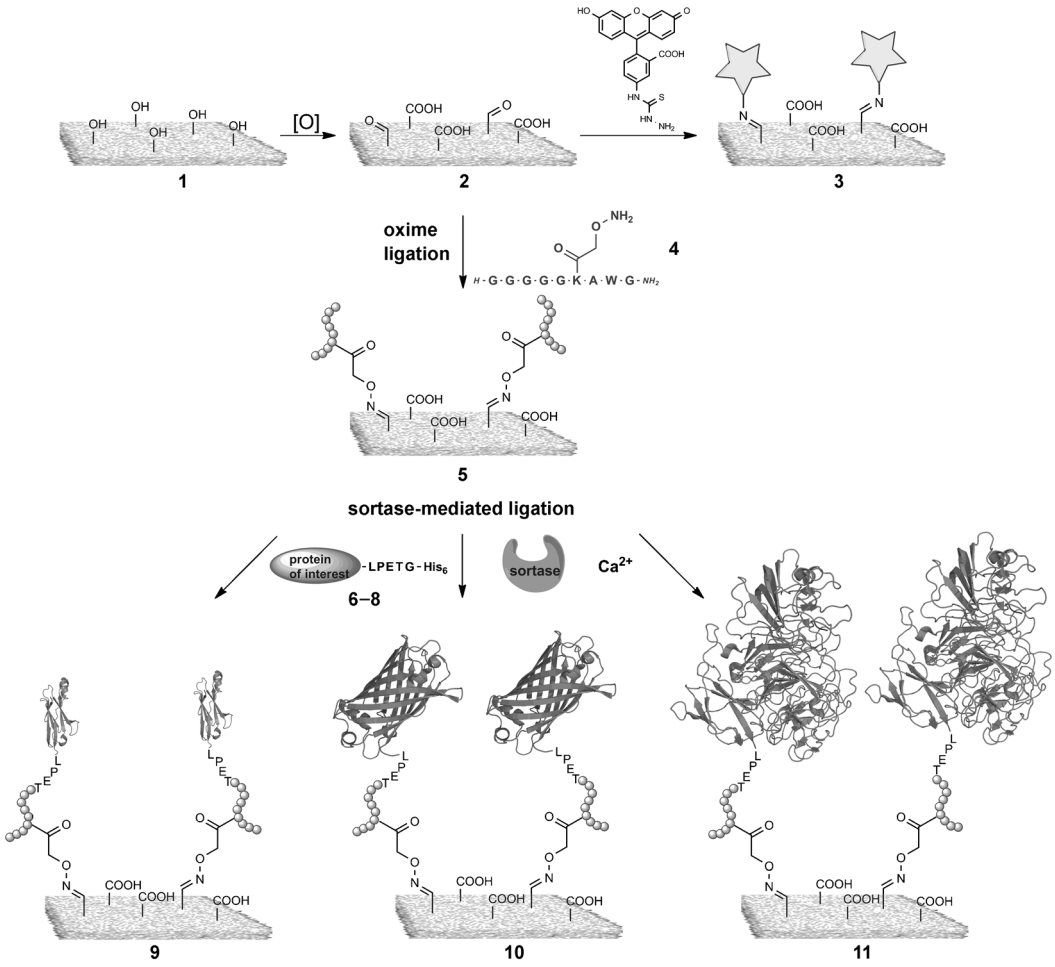

Figure 2. General synthetic strategy. CNC surfaces with the respective groups are shown as gray panels; fluorescein moieties are depicted as stars; peptide **4** is written in one-letter code and schematically drawn as a chain; immobilized proteins are derived from the respective Protein Data Base (PDB) images 2I24, 2WQ8, and 2G6X.

reference sample. These data suggest that modified CNC can be now functionalized with any suitable partner that bears carbonyl-reactive moieties, among them hydrazines, hydrazides, and hydroxylamines. It is important to note that a direct coupling of proteins to aldehyde-bearing CNCs through Schiff base formation with surface-exposed amino groups of lysine residues only occurred to a very low extent (see Figure S12C in the Supporting Information).

To ensure bioconjugation with functional proteins, the surface of carbonyl-bearing CNCs was modified with an oligopeptide module comprising the sortase recognition sequence penta-Gly. To facilitate spectroscopic analysis and purification of peptide **4** (see Figure 2), a tryptophan residue was introduced at the *C*-terminal portion. The linker was covalently attached through a carbonyl-reactive aminooxy group, which was installed through the orthogonally protected side chain of lysine. To this end, the peptide was assembled on Rink amide resin using manual Fmoc-SPPS (see Figure S2 in the Supporting Information) and NHS-activated ethoxyethylidene (Eei)-protected aminooxy acetic acid was coupled to the free ε-amino group of the lysine residue after acidolytic

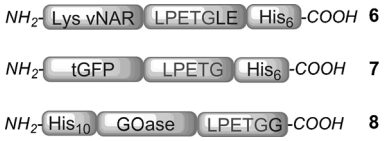

Figure 3. Design of recombinant proteins. **6**: shark antibody Lys-vNAR, **7**: tGFP, **8**: GOase. All proteins comprise the LPETG sortase A recognition sequence as well as His_n tags; $n = 6$ (**6**, **7**) or 10 (**8**).

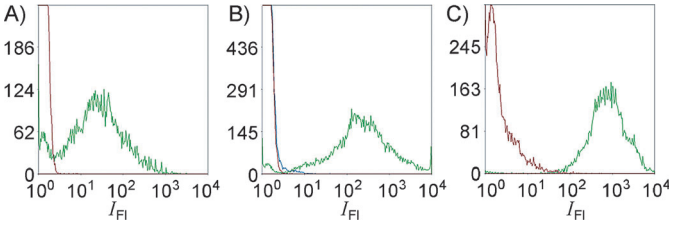

Figure 4. Flow cytometric analysis of CNC conjugates. A) Fluorophore-bearing conjugate **3**; B) tGFP–CNC conjugate **10**; C) Lys-vNAR–CNC conjugate **9**. Red curves: Unlabeled CNCs. Blue curve: CNC lacking the sortase recognition peptide. Green curves: fluorescently labeled CNCs.

On average, the obtained CNCs are smaller than cellulose nanofibrils derived from native cellulose fibers by TEMPO-mediated oxidation.[14,17] This can be explained easily considering that the applied microcrystalline cellulose precursor is in general much smaller than the native counterpart.

To visualize the surface-exposed carbonyl groups, the aldehyde-reactive fluorescein-5-thiosemicarbazide (5FTSC), a fluorescent probe applied in a number of life-science applications, was attached. CNC particles were reacted with 5FTSC in the dark in phosphate-buffered saline (PBS) at ambient temperature, washed, and analyzed by flow cytometry. The diagram in Figure 4A clearly shows the pronounced fluorescent signal of 5FTSC-labeled CNC **3**, compared to the

removal of its methyltrityl (Mtt) protecting group. After the chain assembly was completed, the peptide was cleaved from the resin using a mixture of trifluoroacetic acid (TFA, 92%) and respective scavengers (see Section 1.8 in the Supporting Information) with simultaneous cleavage of all protecting groups.

The peptidic linker **4** was covalently grafted on the CNC surface upon formation of a stable oxime bond in ammonium acetate buffer (pH 4.75).[18] We used 3 equiv of the peptidic module relative to the surface carbonyl groups. According to the elemental analysis (see Table S1 in the Supporting Information), 69% of the surface aldehyde groups were decorated with **4**. After the exchange of reaction buffer for a buffer at physiological pH (7.5) by dialysis or by centrifugation, the modified CNC is ready for the enzyme-mediated biofunctionalization.

Three functional proteins differing in size, shape, and biological activity were chosen for grafting. Our main task was to obtain the CNC molecular constructs bearing functional, fully active proteins that are covalently attached to the CNC surface in a regioselective manner, that is, at their exposed carboxy terminus. Although a number of methods making use of nanocellulose as a platform to graft biological ligands have already been developed,[11b] our novel immobilization format implies highly specific, site-directed covalent coupling, in contrast to commonly used noncovalent and/or random methods.

In the initial experiment we used a 27 kDa derivative of green fluorescent protein (tGFP) which has become a standard tool for "proof-of-concept" protein conjugations due to its pronounced autofluorescence.[19] The second protein used in our study belongs to the family of the smallest known antigen-binding antibody-like domains, namely, the shark variable domains of the New Antigen Receptor, where the antigen-binding site (paratope) is formed by one single domain, referred to as vNAR domain.[20] The 13 kDa Lys-vNAR[21] construct **6** can be detected through the interaction with its fluorescently labeled target, namely, hen egg lysozyme. Since in the present study a modified version of Lys-vNAR bearing an LPETGLE extension was used, maintenance of the binding properties of this construct was verified using biolayer interferometry. To this end, the kinetic parameters of the binding of **6** to hen egg lysozyme were determined giving a K_d value of (4.0 ± 0.16) nM (see Figure S9 in the Supporting Information). Hence, the affinities of the modified Lys-vNAR were consistent with those obtained for its parent molecule.[22] The third model protein used in this study was a 70 kDa galactose oxidase (GOase) enzyme, belonging to the family of oxidoreductases. It utilizes two substrates, D-galactose and oxygen, converting them into hexodialdose and hydrogen peroxide, respectively, that could be easily detected in colorimetric assays.

All three proteins were expressed recombinantly in *E. coli* and were engineered to bear the sortase recognition sequence LPETG *C*-terminally. To facilitate their isolation and purification through affinity chromatography, the proteins were decorated at the *N*- or *C*-terminus with His-tags for convenient purification on Ni-loaded NTA resin (Figure 3). We took an evolved variant of sortase A (referred to as eSrtA) for the conjugations, as it demonstrated enhanced catalytic properties (reaction kinetics) than the wild-type.[23]

A typical protein-grafting experiment was conducted in Tris/NaCl buffer (pH 7.5) containing $CaCl_2$ (5 mM). After overnight reaction the dispersed CNC–protein conjugates **9**, **10**, and **11** (see Figure 2) were isolated from the reaction mixtures by sedimentation and purified by repeated washing (see Section 4 in the Supporting Information). The resulting modified CNCs were analyzed by AFM verifying that the overall length and shape of the nanocellulose particles was maintained, while, depending on the molecular mass of the attached proteins, an increase in particle height was observed (Figure 5). The activity of the immobilized proteins was then examined in the respective assays.

The CNC–tGFP conjugate was analyzed using fluorescence microscopy and flow cytometry. In the initial microscopic study, the tGFP-functionalized nanocellulose whiskers **10** were clearly visible as fluorescent green spots in the micrographs (see Figure S13 in the Supporting Information) indicating that the protein was successfully grafted. Flow cytometry, a well-established technique used to analyze microscopic particles by sensing their optical properties, was used to resolve individual CNCs through probe-conferred fluorescence. Thus, the CNC particles **10** exhibit a fluorescent signal that is about 100 times stronger than that for the reference (unmodified CNC), confirming the attachment of tGFP (Figure 4B). Detailed data of flow cytometric experiments are summarized in Figure S12 in the Supporting Information.

To verify that the shark vNAR has been conjugated with the CNC surface and retained its activity in construct **9**, its binding to the fluorescently labeled target, hen egg lysozyme, was visualized by flow cytometry (Figure 4C). The fluorescence profile showed clear evidence of the protein's activity attributed to the target binding. However, it must be mentioned that the analysis of **9** was more complicated than that of **10**, due to the tendency of lysozyme to form nonspecific interactions with CNCs (see Figure S12C in the Supporting Information).

Oxidation of D-galactose to the respective D-*galacto*-hexodialdose is catalyzed by the enzyme GOase and associated with the formation of hydrogen peroxide. Therefore, the catalytic activity of GOase could be easily monitored by coupling the production of hydrogen peroxide to a horseradish peroxidase catalyzed transformation of ABTS (Figure 6A). A soluble green final product can be detected photometrically at $\lambda = 405$ nm. The analysis of conjugate **11** showed that the immobilized GOase retained its activity upon grafting onto CNC (Figure 6B).

To compare the efficacy of our site-directed coupling strategy compared to the commonly used formation of amide bonds from primary amines of grafted proteins and carboxylic groups of the cellulose support, *N*-hydroxysuccinimide active ester (NHS)-mediated attachment of GOase (the largest protein in our experiments) was conducted. To this end, the proportion of surface carboxylate groups equal to the molar ratio of oximated carbonyl groups was activated by EDC/NHS (see Section 5.1 in the Supporting Information) and reacted with equimolar amount of GOase (the proportions

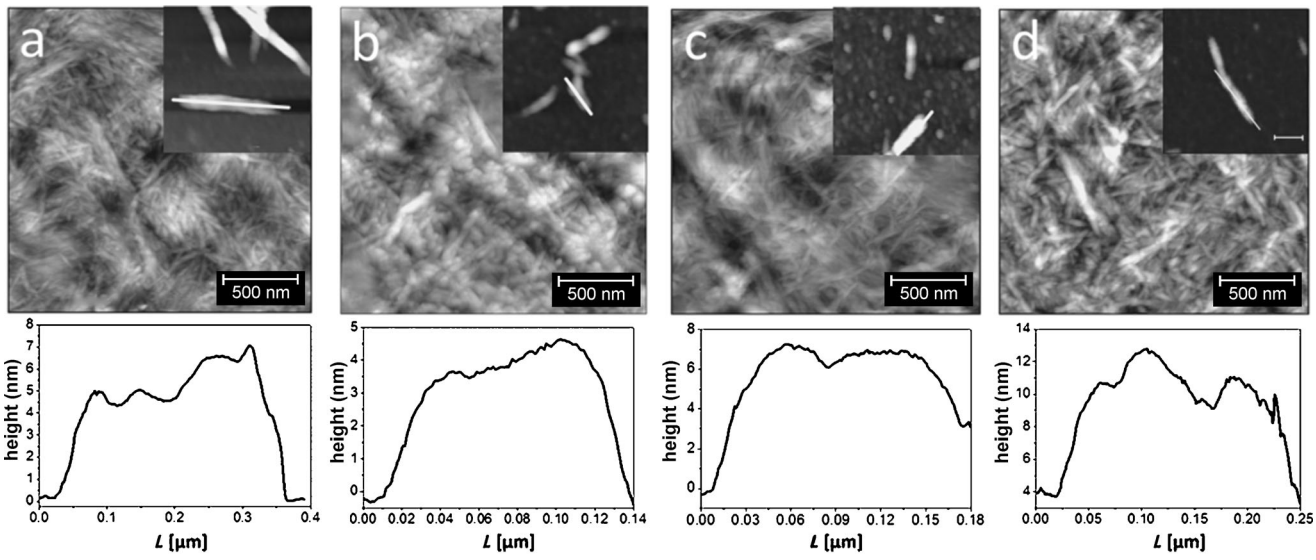

Construct	Height (nm)	Construct	Height (nm)
CNC **2**	5.83±1.13	CNC-tGFP **10**	7.26±0.26
CNC-recognition peptide **5**	5.77±1.07	CNC-GOase **11**	7.72±1.12
CNC-Lys vNAR **9**	6.21±1.15		

Figure 5. Top: AFM images of functionalized CNCs. a) **5** (conjugate with **4**); b) **9** (conjugate with **6**); c) **10** (conjugate with **7**); d) **11** (conjugate with **8**). The insets are magnified images of individual CNCs. The height profiles of the modified CNCs are shown under each AFM image. Bottom: The corresponding heights.

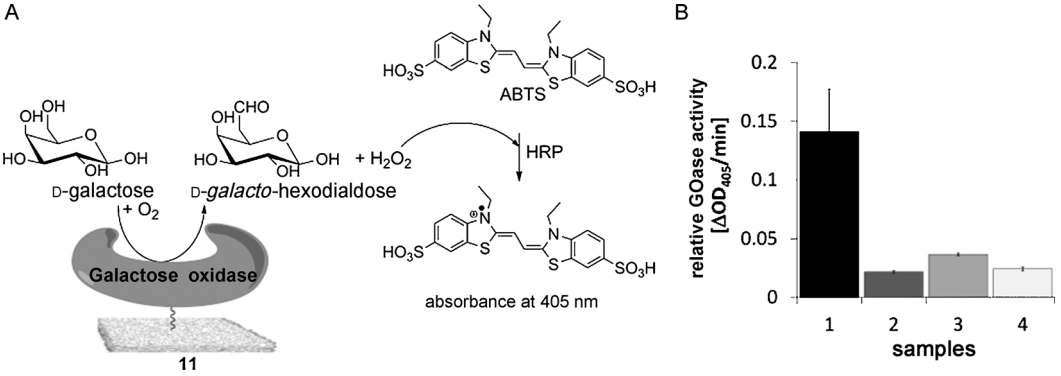

Figure 6. Assessment of the activity of immobilized GOase. A) Schematic depiction of ABTS assay. B) Photometric monitoring of GOase activity in conjugate **11** (1) compared to controls (2: reaction mixture lacking Ca^{2+}, 3: reaction mixture lacking recognition peptide **4**; 4: reaction mixture lacking sortase). Error bars were calculated from a triple determination.

were similar to those for the coupling of peptidic linker **4**). The relative enzyme activity of the immobilized protein was verified using the colorimetric ABTS assay. Thus, compared to the relative GOase activity calculated for the sortase-mediated coupling, the NHS-mediated procedure led to a reduced activity of the surface-immobilized enzyme (ca. 60% of that achieved for the sortase-mediated grafting) (see Figure S10 in the Supporting Information). This outcome could be explained taking into consideration that the NHS-promoted immobilization is random, and all available amino functions of the enzyme are utilized, which could result in restricted access to its active site. On the other hand, the sortase-mediated ligation results in protein-loaded surfaces where all biomacromolecules are grafted exclusively through their *C*-termini (see Figure S11 in the Supporting Information). However, the efficacy of this direct NHS-mediated immobilization also depends on the size and the isoelectric point of the grafted protein and therefore may vary for enzymes other than GOase.

CNC is doubtlessly considered to be a valuable substrate for the deposition of bioactive compounds with different properties. Unlike traditional supports, it provides a large surface area, can be easily prepared from a renewable source, cellulose, and can be chemically modified yielding an extensive nanorelief bearing surface-exposed active groups. The introduction of orthogonally addressable aldehyde units allows for the application of chemical and/or enzymatic methods compatible with biomacromolecules, thus making CNC an advantageous nanoplatform for the immobilization of biological compounds.

We successfully transformed primary alcohols on the surface of CNCs into the respective aldehyde functions,[24] thus enabling the application of highly efficient oxime ligation to immobilize bioactive modules. Since the aldehyde groups are orthogonal to the reactive groups of peptides, we could

couple oligopeptidic motifs that are recognized by the transpeptidase sortase A for further CNC modification by proteins of choice.

Our approach provides a number of obvious advantages over other methods for protein immobilization onto cellulose-derived scaffolds. First, smooth oxidation of surface hydroxy groups to the respective aldehyde units enables orthogonal couplings, ergo, no protection is required upon oxime ligation. Second, sortase-mediated protein grafting takes place under physiological conditions leaving the protein structure, hence activity, intact. Third, the coupling is site-directed, regiospecific, and covalent, and could be easily controlled leading to the formation of tailor-made constructs. Generally, these new G_5-CNCs combine the intrinsic properties of CNC scaffolds, for example low toxicity and water compatibility, with the advantages of recombinantly produced proteins of choice. Moreover, as a cleavable site can be easily installed into recombinant proteins, the controlled detachment of bioactive proteins from the cellulose surface becomes possible, making these conjugates good candidates for, for example, drug deposition and delivery. Of course, our approach is not limited to proteins and could be applied to a vast number of bioactive molecules.

Received: April 23, 2014
Published online: July 28, 2014

Keywords: bioorthogonal protein immobilization · cellulose nanocrystals · enzyme catalysis · immobilization · ligation

[1] D. Klemm, B. Heublein, H. P. Fink, A. Bohn, *Angew. Chem.* **2005**, *117*, 3422 – 3458; *Angew. Chem. Int. Ed.* **2005**, *44*, 3358 – 3393.

[2] a) D. Peschel, K. Zhang, S. Fischer, T. Groth, *Acta Biomater.* **2012**, *8*, 183 – 193; b) H. Jin, M. Kettunen, A. Laiho, H. Pynnonen, J. Paltakari, A. Marmur, O. Ikkala, R. H. A. Ras, *Langmuir* **2011**, *27*, 1930 – 1934; c) G. Y. Yun, J. Kim, J. H. Kim, S. Y. Kim, *Sens. Actuators A* **2010**, *164*, 68 – 73; d) T. Wandowski, P. Malinowski, W. M. Ostachowicz, *Smart Mater. Struct.* **2011**, *20*, 025002; e) D. Sinha, S. Pisana, A. J. Flewitt, *Smart Mater. Struct.* **2011**, *20*, 025016.

[3] a) R. J. Moon, A. Martini, J. Nairn, J. Simonsen, J. Youngblood, *Chem. Soc. Rev.* **2011**, *40*, 3941 – 3994; b) Y. Habibi, L. A. Lucia, O. J. Rojas, *Chem. Rev.* **2010**, *110*, 3479 – 3500; c) D. Klemm, F. Kramer, S. Moritz, T. Lindstrom, M. Ankerfors, D. Gray, A. Dorris, *Angew. Chem.* **2011**, *123*, 5550 – 5580; *Angew. Chem. Int. Ed.* **2011**, *50*, 5438 – 5466.

[4] a) M. Hirota, K. Furihata, T. Saito, T. Kawada, A. Isogai, *Angew. Chem.* **2010**, *122*, 7836 – 7838; *Angew. Chem. Int. Ed.* **2010**, *49*, 7670 – 7672; b) S. C. Espinosa, T. Kuhnt, E. J. Foster, C. Weder, *Biomacromolecules* **2013**, *14*, 1223 – 1230; c) D. Bondeson, A. Mathew, K. Oksman, *Cellulose* **2006**, *13*, 171 – 180; d) K. Abe, S. Iwamoto, H. Yano, *Biomacromolecules* **2007**, *8*, 3276 – 3278.

[5] a) A. P. Mangalam, J. Simonsen, A. S. Benight, *Biomacromolecules* **2009**, *10*, 497 – 504; b) S. Barazzouk, C. Daneault, *Nanomaterials* **2012**, *2*, 187 – 205; c) S. Barazzouk, C. Daneault, *Cellulose* **2012**, *19*, 481 – 493; d) S. Arola, T. Tammelin, H. Setala, A. Tullila, M. B. Linder, *Biomacromolecules* **2012**, *13*, 594 – 603; e) J. V. Edwards, N. Prevost, K. Sethumadhavan, A. Ullah, B. Condon, *Cellulose* **2013**, *20*, 1223 – 1235; f) Y. X. Zhang, R. G. Carbonell, O. J. Rojas, *Biomacromolecules* **2013**, *14*, 4161 – 4168.

[6] a) M. J. Clift, E. J. Foster, D. Vanhecke, D. Studer, P. Wick, P. Gehr, B. Rothen-Rutishauser, C. Weder, *Biomacromolecules* **2011**, *12*, 3666 – 3673; b) X. Yang, E. Bakaic, T. Hoare, E. D. Cranston, *Biomacromolecules* **2013**, *14*, 4447 – 4455.

[7] a) S. Barazzouk, C. Daneault, *Cellulose* **2011**, *18*, 643 – 653; b) S. Barazzouk, C. Daneault, *Cellulose* **2012**, *19*, 481 – 493; c) V. Incani, C. Danumah, Y. Boluk, *Cellulose* **2013**, *20*, 191 – 200; d) M. A. Karaaslan, G. Z. Gao, J. F. Kadla, *Cellulose* **2013**, *20*, 2655 – 2665.

[8] S. V. Rao, K. W. Anderson, L. G. Bachas, *Mikrochim. Acta* **1998**, *128*, 127 – 143.

[9] V. Incani, C. Danumah, Y. Boluk, *Cellulose* **2013**, *20*, 191 – 200.

[10] a) H. Orelma, L. S. Johansson, I. Filpponen, O. J. Rojas, J. Laine, *Biomacromolecules* **2012**, *13*, 2802 – 2810; b) H. Orelma, I. Filpponen, L. S. Johansson, M. Osterberg, O. J. Rojas, J. Laine, *Biointerphases* **2012**, *7*, 61; c) H. Brumer, Q. Zhou, M. J. Baumann, K. Carlsson, T. T. Teeri, *J. Am. Chem. Soc.* **2004**, *126*, 5715 – 5721.

[11] a) D. Rabuka, J. S. Rush, G. W. deHart, P. Wu, C. R. Bertozzi, *Nat. Protoc.* **2012**, *7*, 1052 – 1067; b) M. K. M. Leung, C. E. Hagemeyer, A. P. R. Johnston, C. Gonzales, M. M. J. Kamphuis, K. Ardipradja, G. K. Such, K. Peter, F. Caruso, *Angew. Chem.* **2012**, *124*, 7244 – 7248; *Angew. Chem. Int. Ed.* **2012**, *51*, 7132 – 7136; c) T. Matsumoto, T. Tanaka, A. Kondo, *Langmuir* **2012**, *28*, 3553 – 3557.

[12] a) T. Proft, *Biotechnol. Lett.* **2010**, *32*, 1 – 10; b) M. W. L. Popp, H. L. Ploegh, *Angew. Chem.* **2011**, *123*, 5128 – 5137; *Angew. Chem. Int. Ed.* **2011**, *50*, 5024 – 5032.

[13] J. E. Hudak, R. M. Barfield, G. W. de Hart, P. Grob, E. Nogales, C. R. Bertozzi, D. Rabuka, *Angew. Chem.* **2012**, *124*, 4237 – 4241; *Angew. Chem. Int. Ed.* **2012**, *51*, 4161 – 4165.

[14] T. Saito, A. Isogai, *Biomacromolecules* **2004**, *5*, 1983 – 1989.

[15] a) A. Isogai, T. Saito, H. Fukuzumi, *Nanoscale* **2011**, *3*, 71 – 85; b) K. Zhang, S. Fischer, A. Geissler, E. Brendler, *Carbohydr. Polym.* **2012**, *87*, 894 – 900.

[16] a) S. Dong, M. Roman, *J. Am. Chem. Soc.* **2007**, *129*, 13810 – 13811; b) S. Beck-Candanedo, M. Roman, D. G. Gray, *Biomacromolecules* **2005**, *6*, 1048 – 1054.

[17] T. Saito, S. Kimura, Y. Nishiyama, A. Isogai, *Biomacromolecules* **2007**, *8*, 2485 – 2491.

[18] a) S. Fabritz, S. Hörner, O. Avrutina, H. Kolmar, *Org. Biomol. Chem.* **2013**, *11*, 2224 – 2236; b) A. Dirksen, T. M. Hackeng, P. E. Dawson, *Angew. Chem.* **2006**, *118*, 7743 – 7746; *Angew. Chem. Int. Ed.* **2006**, *45*, 7581 – 7584; c) H. Salo, P. Virta, H. Hakala, T. P. Prakash, A. M. Kawasaki, M. Manoharan, H. Lonnberg, *Bioconjugate Chem.* **1999**, *10*, 815 – 823.

[19] a) T. Misteli, D. L. Spector, *Nat. Biotechnol.* **1997**, *15*, 961 – 964; b) H. Niwa, S. Inouye, T. Hirano, T. Matsuno, S. Kojima, M. Kubota, M. Ohashi, F. I. Tsuji, *Proc. Natl. Acad. Sci. USA* **1996**, *93*, 13617 – 13622.

[20] V. A. Streltsov, J. N. Varghese, J. A. Carmichael, R. A. Irving, P. J. Hudson, S. D. Nuttall, *Proc. Natl. Acad. Sci. USA* **2004**, *101*, 12444 – 12449.

[21] R. L. Stanfield, H. Dooley, M. F. Flajnik, I. A. Wilson, *Science* **2004**, *305*, 1770 – 1773.

[22] H. Dooley, R. L. Stanfield, R. A. Brady, M. F. Flajnik, *Proc. Natl. Acad. Sci. USA* **2006**, *103*, 1846 – 1851.

[23] a) I. Chen, B. M. Dorr, D. R. Liu, *Proc. Natl. Acad. Sci. USA* **2011**, *108*, 11399 – 11404; b) M. W.-L. Popp, J. M. Antos, H. L. Ploegh, *Current Protocols in Protein Science,* Supplement 56, *Unit 15.3*, **2009**; c) C. S. Theile, M. D. Witte, A. E. M. Blom, L. Kundrat, H. L. Ploegh, C. P. Guimaraes, *Nat. Protoc.* **2013**, *8*, 1800 – 1807.

[24] T. Saito, M. Hirota, N. Tamura, S. Kimura, H. Fukuzumi, L. Heux, A. Isogai, *Biomacromolecules* **2009**, *10*, 1992 – 1996.

